Mouse Emi2 is required to enter meiosis II by reestablishing cyclin B1 during interkinesis

Suzanne Madgwick,[1] David V. Hansen,[2,3] Mark Levasseur,[1] Peter K. Jackson,[2,3] and Keith T. Jones[1]

[1]Institute for Cell and Molecular Biosciences, The Medical School, University of Newcastle, Newcastle NE2 4HH, England, UK
[2]Department of Pathology and [3]Program in Cancer Biology, Stanford University School of Medicine, Stanford, CA 94305

During interkinesis, a metaphase II (MetII) spindle is built immediately after the completion of meiosis I. Oocytes then remain MetII arrested until fertilization. In mouse, we find that early mitotic inhibitor 2 (Emi2), which is an anaphase-promoting complex inhibitor, is involved in both the establishment and the maintenance of MetII arrest. In MetII oocytes, Emi2 needs to be degraded for oocytes to exit meiosis, and such degradation, as visualized by fluorescent protein tagging, occurred tens of minutes ahead of cyclin B1.

Emi2 antisense morpholino knockdown during oocyte maturation did not affect polar body (PB) extrusion. However, in interkinesis the central spindle microtubules from meiosis I persisted for a short time, and a MetII spindle failed to assemble. The chromatin in the oocyte quickly decondensed and a nucleus formed. All of these effects were caused by the essential role of Emi2 in stabilizing cyclin B1 after the first PB extrusion because in Emi2 knockdown oocytes a MetII spindle was recovered by Emi2 rescue or by expression of nondegradable cyclin B1 after meiosis I.

Introduction

Oocytes arrest at metaphase of the second meiotic division (MetII) before fertilization because of an activity termed cytostatic factor (CSF; Masui, 2000; Tunquist and Maller, 2003; Jones, 2005). Sperm break this arrest via a Ca²⁺ signal (Jones, 1998; Stricker, 1999; Runft et al., 2002), and in so doing, oocytes complete the second meiotic division before entering the embryonic cell cycles.

CSF activity, a terminology that was first defined several decades ago (Masui and Market, 1971), is now known to constitute an inhibitor of the anaphase-promoting complex/cyclosome (APC; Tunquist and Maller, 2003). The APC is an E3 ubiquitin ligase whose activity is required for the metaphase–anaphase transition to polyubiquitinate key cell cycle proteins, thereby earmarking them for immediate proteolysis through association with its key coactivator cdc20 (Fang et al., 1998; Kramer et al., 1998; Harper et al., 2002; Eytan et al., 2006). The reduced APC^cdc20 activity in MetII oocytes prevents the destruction of

both M-phase (maturation)–promoting factor (MPF) activity (CDK1/cyclin B1) and cohesin, which holds sister chromatids together (Nixon et al., 2002; Madgwick et al., 2004). Resumption of meiosis in mammalian oocytes is achieved by a sperm-borne phospholipase C activity (Saunders et al., 2002; Knott et al., 2005), which generates an oscillatory Ca²⁺ signal, switching on APC^cdc20 (Nixon et al., 2002; Madgwick et al., 2004) through a signaling pathway involving calmodulin-dependent protein kinase II (CamKII; Markoulaki et al., 2003, 2004; Madgwick et al., 2005). This signaling process is conserved and was first demonstrated in frog eggs (Lorca et al., 1993, 1994). Activation of the APC in MetII oocytes induces the destruction of MPF and sister chromatid cohesion through the polyubiquitination of cyclin B1 and securin, respectively (Morgan, 1999; Zachariae and Nasmyth, 1999; Peters, 2002). Loss of cyclin B1 causes a reduction in MPF, and the loss of securin frees separase to act on the kleisin component of cohesin (Zachariae and Nasmyth, 1999; Peters, 2002; Blow and Tanaka, 2005; Nasmyth and Haering, 2005).

Many proteins have been associated with the establishment and/or maintenance of CSF activity. Factors responsible for setting up a second meiotic spindle after completion of meiosis I do not, a priori, have to be the same as those that are responsible for maintaining arrest. Indeed, proteins have been described that are involved in establishing MetII, but not in maintaining arrest once it has been achieved (Tunquist and Maller, 2003).

The mechanism of CSF is most well characterized in the frog, where various groups have firmly defined the c-Mos–MAPK–90-kD ribosomal protein S6 kinase (p90rsk)–budding uninhibited by benzimidazole 1 (Bub1) pathway in establishing CSF activity (Sagata et al., 1989; Abrieu et al., 1996; Bhatt and Ferrell, 1999; Gross et al., 1999, 2000; Tunquist et al., 2002). Other activities that are fundamentally involved in the establishment of CSF in frog include cyclin E/Cdk2 (Tunquist et al., 2002) and mitotic arrest deficient 2 (Mad2; Tunquist et al., 2003). However, once established, p90rsk, Mad2, Bub1, and cyclin E/Cdk2 are all dispensable for the maintenance of CSF activity (Bhatt and Ferrell, 1999; Tunquist et al., 2002, 2003).

So, how is CSF activity maintained in the frog? Current evidence suggests it is through early mitotic inhibitor 2 (Emi2)/Emi-related protein 1 (Liu and Maller, 2005; Rauh et al., 2005; Schmidt et al., 2005; Tung et al., 2005; Hansen et al., 2006). Emi2, which acts to inhibit the APC accumulated during oocyte maturation, is present and stable in CSF frog egg extracts, but is rapidly degraded on Ca^{2+} addition (Schmidt et al., 2005). Degradation of Emi2 is induced by phosphorylation through CamKII (Liu and Maller, 2005; Rauh et al., 2005; Hansen et al., 2006) and, thus, would be predicted to occur ahead of APC activation and cyclin B1 degradation, although this has not been tested.

In mouse oocytes, the mechanism of CSF arrest is less well understood. As the mouse Emi2 homologue appears to have a similar function in maintaining CSF activity (Shoji et al., 2006), it would be logical to predict that the mechanism of CSF establishment is also conserved between frog and mouse. However, this is not so. Oocytes from a triple Rsk (1,2,3) knockout mouse arrest normally at MetII (Dumont et al., 2005), demonstrating that p90Rsk is not involved in mouse CSF arrest. Furthermore, using dominant-negative mutants Tsurumi et al., (2004) confirmed that the spindle checkpoint proteins Bub1 and Mad2 are not required for either the establishment or the maintenance of mouse CSF. Although c-Mos is known to be involved in CSF maintenance, it does not appear to be involved in the establishment of CSF arrest because c-Mos −/− oocytes remain at MetII for 2–4 h before extruding a second PB (PB2; Verlhac et al., 1996).

As there are no firm candidates suggested to be involved in the establishment of CSF arrest in mouse, we have investigated the potential of mouse Emi2 in this process. We find that Emi2 has activity consistent with CSF, and its degradation in real time is ahead of any change in cyclin B1. We also demonstrate that a function of Emi2 is in restabilizing cyclin B1 upon exit from anaphase I and that, in this study, it contributes to the formation a bipolar spindle. Oocytes matured without Emi2 do not assemble MetII spindles, and, in the absence of cyclin B1, eventually decondense their chromatin.

Results

Stable Emi2 is rapidly degraded by Ca^{2+}

To measure real-time changes in Emi2 levels in oocytes we generated cRNA to mouse Emi2 coupled to Venus fluorescent protein (Emi2-V), which is a yellow variant of GFP. MetII mouse oocytes were microinjected with this construct at a dose of either 0.15 or 0.5 pg, and then cultured for a few hours to allow for Emi2 expression. We Western blotted oocytes expressing Emi2-V with a polyclonal antibody against Emi2 to determine the amount of Emi2-V expression relative to endogenous protein. More than one band was detected on oocyte blots using this antibody; however, one band at ~85 kD migrated at the same molecular mass as in vitro–translated Emi2 (and this band was later knocked down by Emi2 morpholino [MO]). At the 0.15-pg dose, Emi2-V levels were less than endogenous protein after 2 h, whereas the 0.5-pg dose was expressed to about the same level as endogenous protein (Fig. 1 A).

Emi2-V was very stable in MetII-arrested oocytes, but became rapidly unstable when cytosolic Ca^{2+} increased. With either 0.15 pg (Fig. 1 B) or 0.5 pg (not depicted) injections, we observed no degradation of Emi2-V in MetII oocytes after blocking further synthesis by washing into cycloheximide-containing media. However, when this experiment was repeated, but by washing into Sr^{2+}-containing media to induce spermlike Ca^{2+} spiking (Bos-Mikich et al., 1997), we observed dose-dependent effects on Emi2-V. At the higher 0.5-pg dose, we observed no loss in Emi2-V signal; instead, Emi2-V levels steadily increased

Figure 1. **Emi2-V is stable in MetII oocytes, but is rapidly degraded by Ca^{2+}.** (A) Western blot of oocytes microinjected 2 h before with 0.15 or 0.5 pg of Emi2-V. 35 oocytes were loaded per lane. Endogenous Emi2 and Emi2-V are marked. *, nonspecific band. (B) Emi2-V (0.15 pg cRNA) expression levels on addition of cycloheximide (CHX; $n = 12$). (C and D) Emi2-V (C, 0.5 pg cRNA; D, 0.15 pg cRNA) expression levels after washing into Sr^{2+} media at the times indicated (C, $n = 14$; D, $n = 15$). (E) Cyclin B1-V (0.09 pg cRNA) expression levels after washing into Sr^{2+} media at the times indicated ($n = 15$). T_E and T_C represent the time from complete degradation of the Venus fluorochrome (T_E, Emi2; T_C, cyclin B1) to PB2 extrusion in oocytes. PB2 was observed at the times indicated. A is representative of two independent Western blots. (B–E) are representative traces of n oocytes that have been used from two to four independent experiments.
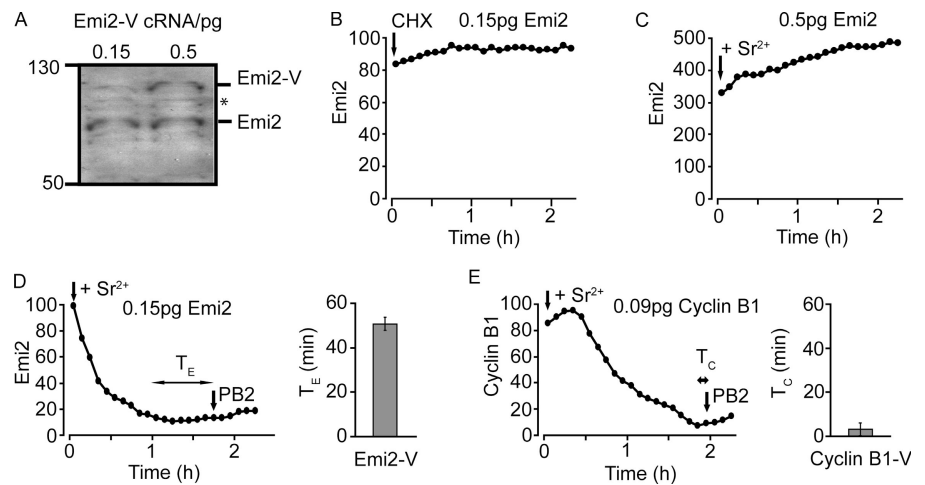
(Fig. 1 C). However, at the lower 0.15-pg dose Emi2-V was rapidly degraded (Fig. 1 D).

The high dose of Emi2 maintained oocytes in a MetII arrest. Oocytes injected with 0.5 pg Emi2-V cRNA showed no morphological signs of meiotic resumption, which is consistent with the maintained Emi2-V levels in these oocytes (Fig. 1 C). In contrast, oocytes that had been injected with 0.15 pg Emi2-V cRNA extruded a PB2 (Fig. 1 D). This suggests that Emi2-V has physiological CSF activity and that the oocyte has a finite capacity to degrade Emi2.

Emi2 is degraded ahead of cyclin B1

At the lower dose Emi2 injection, where we observed Emi2-V degradation, the minimum in its degradation profile after activation with Sr^{2+} media was reached tens of minutes before PB2 extrusion (Fig. 1 D, T_E). However, we have previously reported that cyclin B1 degradation, visualized by coupling to GFP, is only completed at the time of PB2 formation (Hyslop et al., 2004). This suggests that the Emi2 and cyclin B1 degradation profiles may not fully overlap. When cyclin B1 was expressed in mouse oocytes with the same fluorescent protein tag as Emi2 (cyclin B1-Venus; cyclin B1-V), we observed the same degradation profile as that previously found for cyclin B1-GFP, such that a minimum in the cyclin B1-V profile was reached within minutes of PB2 extrusion (Fig. 1 E, T_c).

Comparing the degradation profiles of Emi2-V and cyclin B1-V suggests that Emi2 degradation is initiated ahead of cyclin B1. Sr^{2+}-induced Emi2 degradation begins immediately (Fig. 1 D), whereas that of cyclin B1 begins 20 min later (Fig. 1 E). This would have to occur if MetII arrest is being mediated by Emi2-induced inhibition of APC^{cdc20} activity. Therefore, we wanted to

confirm the immediate loss of endogenous Emi2 signal in oocytes, which is especially important given that Shoji et al. (2006) had reported very little loss in Emi2 signal at a 6-h time point after activation with Sr^{2+}. Oocytes were activated by washing into Sr^{2+} media, and samples from a pool of oocytes were removed at various time points and probed for either cyclin B1 or Emi2 by Western blotting (Fig. 2 A). In these experiments, it was apparent that loss in Emi2 protein was rapid and complete by 30 min (in agreement with the rapid loss of Emi-V shown in Fig. 1 D). Interestingly, Emi2 levels increased again in pronucleate embryos (6-h time point), which is in agreement with Shoji et al. (2006) and suggests that it may have a further mitotic function (see Discussion). Similar to Emi2, we observed the loss of cyclin B1 at 30 min, as well as increased levels in pronucleate embryos (Fig. 2 A), which is consistent with our observation that the APC is switched off at this time (Nixon et al., 2002).

Because of the numbers of oocytes needed for Western blots and the tens of minutes of asynchrony in timing at which Ca^{2+} spiking starts with Sr^{2+} media, (Madgwick et al., 2004), we could not reproducibly resolve Emi2 degradation ahead of cyclin B1 by Western blotting groups of oocytes. Therefore, to examine with more accuracy the immediate degradation profiles of cyclin B1 and Emi2, we decided to measure their simultaneous degradation in the same oocyte. Cyclin B1 was coupled to Cerulean fluorescent protein (cyclin B1-C), which is a cyan variant of GFP. There was no overlap in Venus and Cerulean signals, showing that both Emi2-V and cyclin B1-C, with appropriate filters, could be imaged simultaneously in the same oocyte (Fig. 2 B). In these experiments, it was evident that the introduction of Emi2-V delayed cyclin B1 degradation (Fig. 1 E and Fig. 2 C), which is consistent with Emi2-inhibiting APC
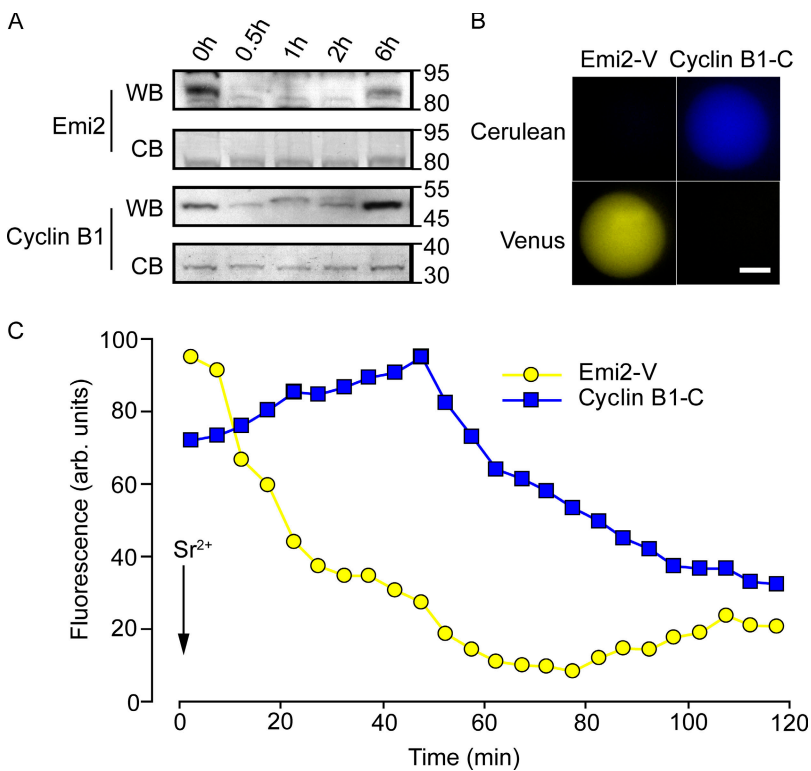

Figure 2. **Emi2 is degraded ahead of cyclin B1.** (A) Western blot (WB) of oocytes for Emi2 (top; $n = 100$ oocytes per lane) and cyclin B1 ($n = 30$ oocytes per lane), and corresponding membranes stained with Coomassie brilliant blue (CB) to show equivalent loading. Oocytes are activated by washing into Sr^{2+} media for the times indicated. (B) Epifluorescence images of MetII oocytes microinjected with Emi2-V cRNA or cyclin B1-C cRNA, at the excitation wavelengths of Cerulean (430 nm) and Venus (500 nm). There is negligible overlap in signal between the two fluorochromes, demonstrating that Emi2-V and cyclin B1-C may be imaged in the same oocyte. Bar, 20 μm. (C) Simultaneous Venus (yellow) and Cerulean (blue) fluorescence in a MetII oocyte expressing Emi2-V and cyclin B1-C, and washed into Sr^{2+} media at time $t = 0$ min. Emi2-V degradation begins tens of minutes before that of cyclin B1. (A) The Western blot was repeated once with similar timings. C is representative of seven oocytes from two independent experiments.
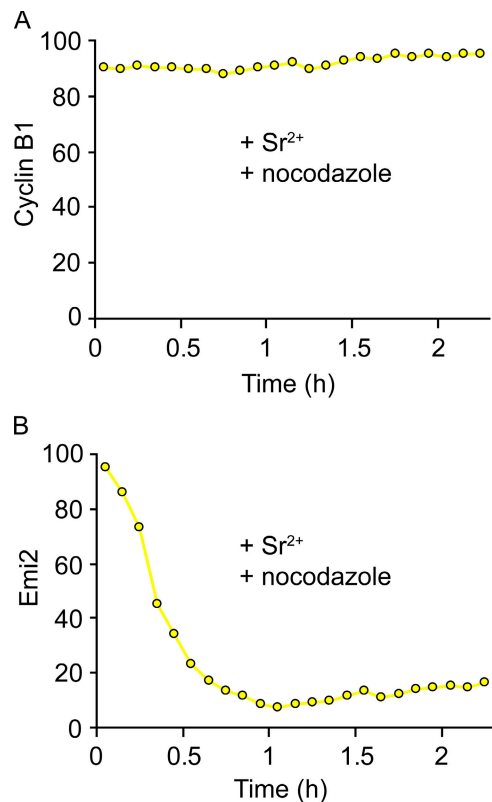
Figure 3. **Emi2-V degradation is independent of a spindle checkpoint.** Venus fluorescence levels in a MetII oocyte expressing cRNA to cyclin B1-V (A; $n = 12$) or Emi2-V (B; $n = 15$) after the addition of Sr^{2+} media containing 100 ng/ml nocodazole at time $t = 0$ h. Both A and B are representative of oocytes collected in two independent experiments.

activity. However, these coexpression studies revealed that Emi2 degradation began tens of minutes before that of cyclin B1 (Fig. 2 C). Emi2-V levels were degraded by at least 50% before the start of cyclin B1-C degradation ($n = 7$).

Emi2 degradation is independent of a spindle checkpoint

Degradation of cyclin B1 is dependent on APC[cdc20] activity, and in mouse oocytes it can be blocked by the induction of a spindle checkpoint (Nixon et al., 2002; Madgwick et al., 2005). In contrast, Emi2 degradation should be checkpoint-independent because its degradation is independent of APC[cdc20] involvement. Incubation of Emi2- and cyclin B1-expressing oocytes with the spindle poison nocodazole blocks mouse oocytes from exiting MetII arrest when washed into Sr^{2+} media. As expected, the addition of nocodazole completely stabilized cyclin B1 levels ($n = 15/15$; Fig. 3 A). However, nocodazole had no effect on the rate of Emi2-V degradation ($n = 12/12$; Fig. 3 B). Such an observation is consistent with cyclin B1, but not Emi2 degradation, being dependent on the APC.

Therefore, in summary, we have obtained data that are entirely consistent with a model of MetII arrest achieved by Emi2-mediated inhibition of cyclin B1 degradation. Also, the Emi2-V construct generated is a physiologically active, useful tool for both establishing CSF activity and measuring its loss in real time after a Ca^{2+} signal.

Oocytes with Emi2 knockdown extrude a PB, but do not MetII arrest

Emi2 levels are low in both *Xenopus laevis* and mouse oocytes before they are matured. This would be predicted, as high Emi2 levels during maturation may be deleterious and arrest oocytes at MetI. The increased Emi2 expression during oocyte maturation makes it highly likely that Emi2 expression can be knocked out by an antisense approach. Therefore, we designed an antisense MO to the 5′UTR immediately adjacent to the start codon of mouse Emi2 (Emi2 MO) and used an additional two MO's as controls (Table I); a 5-base mispair MO (5mp-MO), in which five bases have been altered from the complementary sequence, and an inverted MO (Inv-MO).

To explore the role of Emi2 in the establishment of MetII arrest, we injected Emi2 MO into germinal vesicle (GV) oocytes, which were then matured in vitro. Oocytes were held at the GV stage in milrinone-containing media for 2 h after MO injection; they were then released from GV arrest and allowed to mature for 16 h. Blotting of GV-stage oocytes, Emi2 MO–matured oocytes, and uninjected control matured oocytes demonstrated that Emi2 protein levels increase between GV and MetII stage, and confirmed the Emi2 knockdown in Emi2 MO–injected oocytes (Fig. 4 A).

During maturation, oocytes were scored for the morphological events of oocyte maturation, which are GV breakdown (GVBD) and PB1 extrusion (Fig. 4 B). Both GVBD (Fig. 4 C) and PB1 extrusion (Fig. 4 D) occurred with normal timings in Emi2 MO–injected oocytes. However, after maturation, we observed marked differences in the morphology of control oocytes and those injected with Emi2 MO. When control oocytes (uninjected, 5mp-MO, and Inv-MO–injected) were stained for chromatin, oocytes were morphologically normal. They had a PB1 containing chromatin, which was produced on completion of the first meiotic division, and a fully formed MetII spindle (100%; uninjected oocytes, $n = 60$; 5mp-MO, $n = 32$; Inv-MO, $n = 25$; Fig. 5 A). However, although oocytes injected with Emi2 MO did have a PB1 containing chromatin, the chromatin in the oocyte was decondensed inside a nucleus (93%; $n = 110$; Fig. 5 A).

Despite the lack of effect of a 5mp-MO, it remained possible that we had been extremely unlucky in the MO design, such that the observed effects of Emi2 MO were caused by its ability to block the expression of an unrelated protein involved in MetII arrest. We thought this unlikely, given that a similar morphology of Emi2 knockdown oocytes has been reported recently using a double-stranded RNAi approach (Shoji et al., 2006).
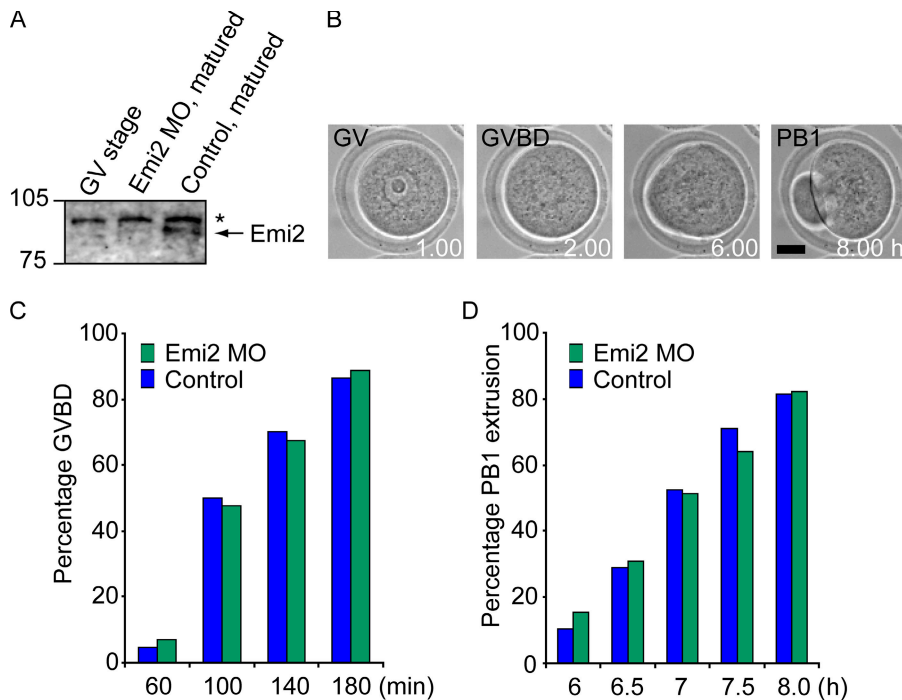
Figure 4. **GVBD and PB1 extrusion occur normally in Emi2 MO–injected oocytes.** (A) Western blot of GV-stage, Emi2 MO–matured, and control matured oocytes; 75 oocytes were loaded per lane. *, nonspecific band. (B) Brightfield time lapse of an oocyte microinjected with Emi2 MO and allowed to mature. GVBD and PB1 are marked. Bar, 20 μm. The percentage rate of GVBD (C) and PB1 extrusion (D) at the times indicated for control oocytes (n = 32) and oocytes microinjected with Emi2 MO (n = 33). The Western blot in A is representative of two independent experiments. The data in C and D was pooled from two independent experiments.

However, we decided it was important to confirm the specificity by a rescue to the control phenotype in Emi2-MO–injected oocytes by expression of exogenous Emi2. To recover Emi2, Emi2-V cRNA was microinjected into oocytes 2 h after microinjection of Emi2 MO and immediately before release from GV arrest. This rescue is made possible because Emi2-V lacks the 5′UTR recognized by the MO.

Injection of Emi2-V cRNA alone into GV oocytes that were matured induced a MetI arrest (n = 40; Fig. 5 A), which is consistent with Emi2-V having CSF activity and the need to keep Emi2 levels low until completion of the first meiotic division. Importantly, Emi2-V cRNA expression could rescue the effects of MO knockdown. Rescue oocytes could progress through meiosis I and arrest as controls with a fully formed MetII spindle. A high dose of Emi2-V (0.5 pg; n = 45) rescued the Emi2 MO phenotype, with an equal mix of either MetI or MetII arrest, whereas oocytes microinjected with the lower Emi2 dose showed a rescue with a predominantly MetII arrest (n = 45; Fig. 5 A).

Lack of Emi2 results in a failure to assemble a metaphase II spindle

By scoring oocytes for decondensed chromatin at only one time point (16 h), we were unable to pinpoint at which stage of meiosis oocytes undergo chromatin decondensation. However, we noted that the vast majority of oocytes with decondensed chromatin extruded only a single PB and contained only one nucleus (88%; n = 102). This observation suggests either decondensation of chromatin occurred after anaphase I, such that oocytes did not form a MetII spindle (Fig. 5 B, i), or, alternatively, that after establishment of a MetII spindle there was no sister chromatid disjunction before decondensation (Fig. 5 B, ii).

We determined whether Emi2 MO knockdown oocytes were able to build a MetII bipolar spindle by staining oocytes for both chromatin and tubulin at various times after PB1 extrusion. Oocytes were fixed at 0.5, 1, and 2 h after PB1 extrusion. In control uninjected oocytes, central spindle microtubules were observed at 0.5 h after PB extrusion (Fig. 6 A), and over the next 1.5 h a MetII spindle formed, such that by 2 h after PB1 a fully formed MetII spindle was found in all oocytes (Fig. 6 B). In Emi2-MO–injected oocytes, at 0.5 h after PB1 there was no difference from controls, with central spindle microtubules evident between the chromatin in the ooplasm and the PB1 (Fig. 6 A). However, in contrast to control oocytes, in Emi2-MO–injected oocytes at both the 1 and the 2 h time points we observed no MetII spindle; instead, the chromatin had remained essentially unaltered from the time of PB1 extrusion. The residual central spindle microtubules remained between the chromatin in the oocyte and the PB, and by 2 h the chromatin appeared to be beginning to decondense (Fig. 6 B). As the chromatin started to decondense, spindle microtubule structure was lost, which is consistent with entry into interphase. By 6 h, all Emi2-MO–injected oocytes had a single nucleus containing fully decondensed chromatin. We did not assess if these oocytes underwent S-phase; however, they showed no obvious signs of degeneration over the 6-h time period from PB1 extrusion. Thus, we failed to observe the formation of a bipolar spindle in any Emi2-MO–treated oocytes; instead, oocytes underwent full chromatin decondensation.

Emi2 stabilizes cyclin B1 after PB1 extrusion

Because the formation of a MetII spindle requires an increase in the levels of CDK1 activity after PB1 extrusion, we reasoned that in the absence of Emi2, levels of CDK1's regulatory partner
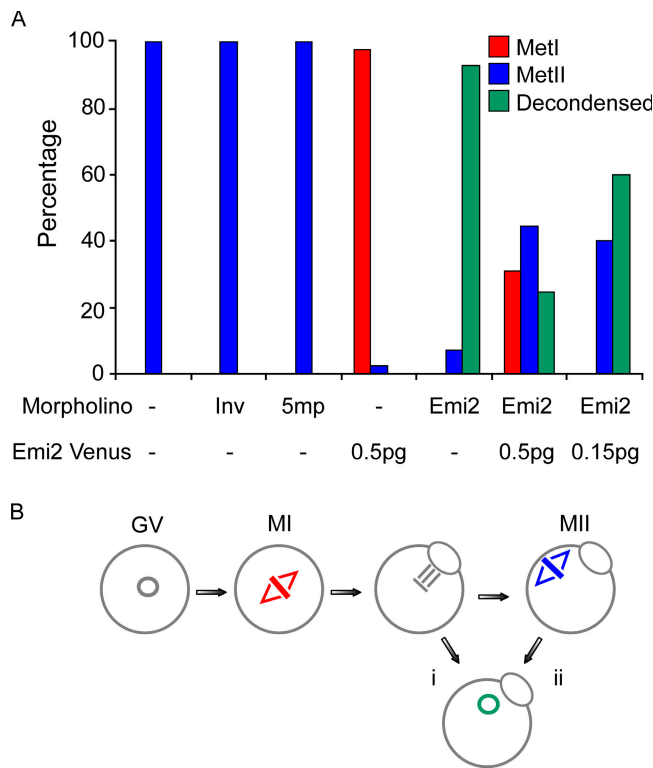
Figure 5. **Decondensed chromatin in Emi2 MO–injected matured oocytes.** (A) Percentage of maturation rates in in vitro–matured oocytes after micro-injection at the GV stage of MOs and/or Emi2-V cRNA, as indicated. Oocyte maturation was assessed at 16 h after release from GV arrest. Oocytes were stained with Hoechst and scored as either arrested at MetI or MetII or as having decondensed chromatin. (B) Emi2 MO oocytes typically extruded a PB1 and contained only one nucleus (88%; n = 102). This single nucleus must result through chromatin decondensation either immediately after PB1 extrusion (i) or after the formation of a MetII spindle that fails to segregate its sister chromatids (ii). The data in A was pooled from 12 independent experiments. See Oocytes with Emi2 knockdown extrude a PB, but do not MetII arrest.

Figure 6. **A bipolar MetII spindle does not form in Emi2 MO–injected oocytes.** Tubulin (red) and chromatin (blue) staining in either Emi2 MO–microinjected or control oocytes at 0.5 (A), 2 (B), or 6 h (C) after PB1 extrusion. (A) In control and Emi2 MO–injected oocytes, a central spindle forms between segregated homologues at 0.5 h. (B) By 2 h after PB1 extrusion, all control oocytes had a bipolar MetII spindle; however, Emi2 MO oocytes showed only microtubules that remained from the persistence of the central spindle. (C) By 6 h after PB1, chromatin in Emi2 MO–injected oocytes had completely decondensed inside a nucleus (N). Bar, 20 μm. Each image is representative of at least 10 oocytes. A–C are representative of two, three, and seven independent experiments, respectively.

cyclin B1 may not be reestablished. To test this directly, Emi2 MO or control GV oocytes were microinjected with cyclin B1-V cRNA and matured in vitro. Cyclin B1-V levels were monitored in real time during maturation, along with brightfield microscopy to assess progression through meiosis I. As previously reported (Hyslop et al., 2004), in control oocytes there was a period of cyclin B1 degradation that lasted a few hours and was terminated on PB1 extrusion (Fig. 7 A). Immediately after PB1 extrusion in these oocytes, cyclin B1 levels rose to 24.0 ± 1.1% (n = 14) of the peak level before PB1 extrusion (Fig. 7 B). In Emi2-MO–injected oocytes, there was no difference from controls in the timing of initiation or in the rate of cyclin B1-V degradation during meiosis I, which is in agreement with the observed lack of effect of the MO on the timing of PB1 (Fig. 4 D). However, in these Emi2 MO oocytes there was no reelevation of cyclin B1 after PB1 extrusion; cyclin B1-V levels increased to just 1.6 ± 0.3% (n = 15) of the peak level before PB1 extrusion (Fig. 7 B).

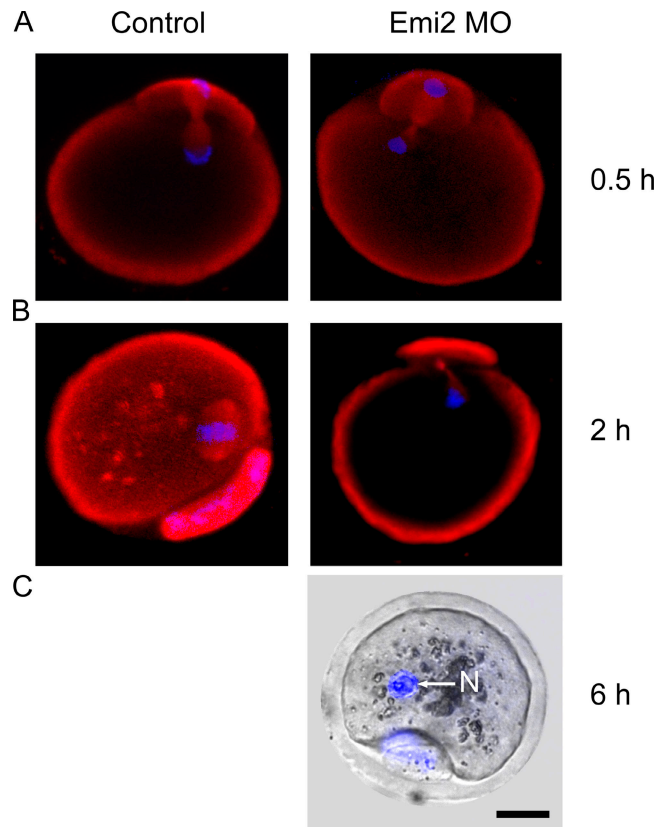In keeping with the real-time effects on exogenous cyclin B1-V expression, we also observed a loss of endogenous cyclin B1 after Emi2 knockdown. In vitro–matured oocytes injected with Emi2 MO at the GV stage showed much lower cyclin B1 levels than control in vitro–matured oocytes (Fig. 7 C). Furthermore, cyclin B1 levels in individual oocytes were measured by immunofluorescence at 16 h after release from GV arrest in control and Emi2-MO–injected oocytes (Fig. 7, D and E). We found that cyclin B1 immunofluorescence levels in Emi2 MO–treated oocytes was about one third that of control oocytes (Fig. 7 E), suggesting a relatively uniform level of knockdown.

Nondegradable cyclin B1 and Mad2 rescue a bipolar spindle in Emi2 knockdown oocytes

Because the formation of a MetII spindle requires an elevation in the levels of cyclin B1, we reasoned that the Emi2 MO spindle defect may be recovered by the addition of cRNA to non-degradable cyclin B1. Furthermore, it should also be rescued by inhibiting the APC^cdc20 by addition of Mad2. Cyclin B1 with deletion of 90 N-terminal amino acids (Δ90 cyclin B1) lacks a D-box and is therefore not a substrate of the APC (Glotzer et al., 1991; Madgwick et al., 2004). Emi2-MO–injected oocytes
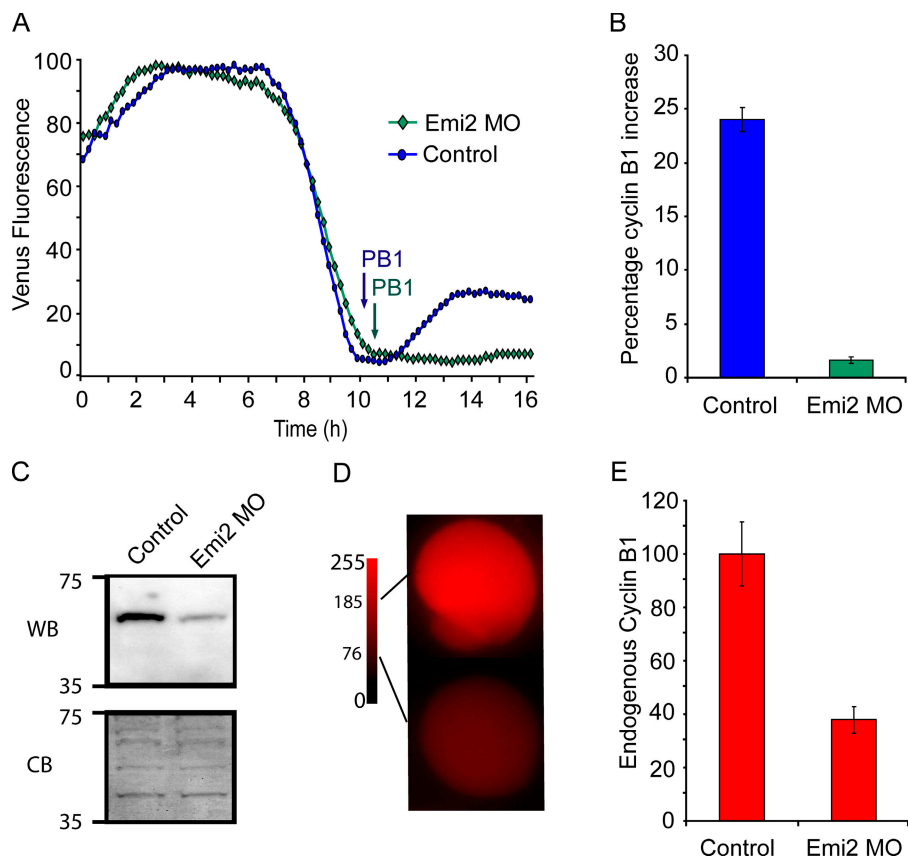
Figure 7. **Cyclin B1 levels remain low after PB extrusion in Emi2 MO–matured oocytes.** (A) Venus fluorescence levels in maturing oocytes microinjected with cyclin B1-V cRNA (control) or cyclin B1-V cRNA and Emi2 MO. PB1 extrusion was observed at the times indicated. Note the similar profile of cyclin B1-V degradation in both oocytes, but the failure of cyclin B1-V levels to rise in the oocyte injected with Emi2 MO after PB1. (B) Quantification of the elevation in cyclin B1-V levels after PB1 extrusion in the control oocytes ($n = 14$) and Emi2 MO oocytes ($n = 15$) used in A. Endogenous cyclin B1 levels in matured oocytes detected by Western blotting (C) or immunofluorescence (D and E). (C) A Western blot (WB) for cyclin B1 in control matured oocytes and oocytes matured after microinjection of Emi2 MO at the GV stage ($n = 40$), and the corresponding membrane stained with Coomassie brilliant blue (CB) to demonstrate equivalent loading. In D, representative images of cyclin B1 levels in matured oocytes (control) and in matured oocytes microinjected at the GV stage with Emi2 MO detected using a TRITC-conjugated secondary antibody. Mean fluorescence readings are marked for both oocytes on the 8-bit scale bar. (E) Quantification of cyclin B1 immunofluorescence levels in control ($n = 25$) and Emi2 MO–microinjected ($n = 32$) oocytes from D, relative to uninjected controls. A is representative of four independent experiments whose data is pooled in B. (C) The Western blot was repeated once. D is representative of two independent experiments whose data is pooled in E.

either received no further treatment or were microinjected with 1.5 pg Δ90 cyclin B1 or Mad2 cRNA within 15 min of PB1 extrusion. This injection had to be done immediately after PB1 extrusion because nondegradable cyclin B1 addition to oocytes before PB1, as predicted by the sustained MPF activity, blocks PB extrusion (Herbert et al., 2003). A few hours of Δ90 cyclin B1 cRNA expression generates cyclin B1 at a similar level to endogenous cyclin B1 in a MetII oocyte (Madgwick et al., 2004). This dose of Mad2 causes a metaphase I arrest in maturing oocytes (Homer et al., 2005) and prevents completion of meiosis in MetII oocytes (Madgwick et al., 2005). At 2 h after PB1 extrusion, all oocytes were fixed, stained, and scored for the presence of a bipolar spindle (Fig. 8 A). As observed in Fig. 6 B, oocytes microinjected with Emi2 MO gave decondensing chromatin with a lack of any bipolar spindle structure. However, as with uninjected oocytes, we observed a fully formed bipolar MetII spindle in oocytes microinjected with Emi2 MO and either Δ90 cyclin B1 cRNA or Mad2 (Fig. 8 B).

Discussion

We have demonstrated in live oocytes and in real time that upon a Ca^{2+} signal, Emi2 degradation occurs ahead of cyclin B1, independent of APC inhibition. The current study confirmed
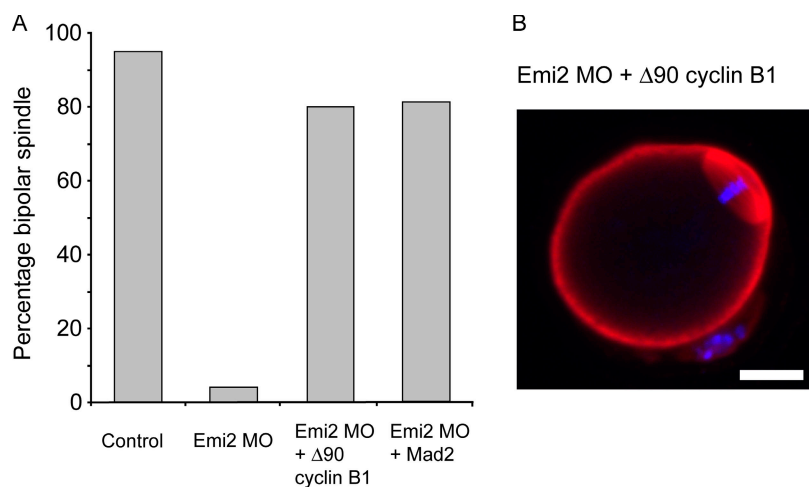
Figure 8. **Emi2 MO phenotype recovery using Δ90 cyclin B1 or Mad2.** (A) Percentage maturation rates in in vitro–matured oocytes after no treatment ($n = 12$), or microinjection of Emi2 MO at the GV stage with or without further microinjection of Δ90 cyclin B1 or Mad2 after PB1 extrusion (Emi2 MO only, $n = 20$; with Δ90 cyclin B1, $n = 25$; or with Mad2, $n = 35$). Oocytes were fixed and stained 2 h after PB1 extrusion and scored for a bipolar spindle. (B) Tubulin (red) and chromatin (blue) staining in an oocyte microinjected with Emi2 MO at the GV stage and then Δ90 cyclin B1 cRNA 15 min after PB1 extrusion. Image is representative of 20/25 oocytes. Bar, 20 μm. Data is pooled from two independent experiments.

that Emi2 constitutes CSF activity in mouse MetII oocytes and is responsible for the maintenance of MetII arrest (Shoji et al., 2006). More importantly, we find that Emi2 is necessary and sufficient in stabilizing cyclin B1 levels at the completion of meiosis I, and such stabilization is essential in establishing a bipolar spindle.

By definition, CSF activity must accumulate during oocyte maturation, inhibit APC^{cdc20} activity at MetII, and be inactivated on a Ca^{2+} signal at fertilization. Although only recently identified, the F-box protein Emi2 is very likely to constitute CSF in frog eggs (Liu and Maller, 2005; Rauh et al., 2005; Schmidt et al., 2005; Tung et al., 2005; Hansen et al., 2006). Emi2 inhibits the ubiquitin ligase activity of the APC^{cdc20} in vitro, and in keeping with the nature of CSF, it accumulates during oocyte maturation, is present in CSF extracts, and is rapidly degraded by Ca^{2+} (Schmidt et al., 2005).

Maintenance of MetII arrest

We tested the characteristics of the mouse Emi2 homologue in MetII mouse oocytes. This achieved two goals. First, it allowed us to demonstrate that Venus-tagged Emi2 is physiologically active, and second, it provided us with data relating to the timing of Emi2 degradation on activation. Excess *X. laevis* Emi2 protein prevents Ca^{2+}-induced CSF release in egg extracts (Schmidt et al., 2005); similarly, our MetII-arrested mouse oocytes were refractory to Ca^{2+} through modest rises in Emi2-V. A lower Emi2-V dose, less than endogenous protein, did not block escape from MetII arrest and allowed us to demonstrate that Emi2 is degraded ahead of cyclin B1. If Emi2 inhibits the APC in MetII arrest, it follows that Emi2 destruction must occur before the APC's accelerated degradation of cyclin B1. Indeed, when both were simultaneously imaged in an oocyte after a Ca^{2+} rise, Emi2 was degraded by at least 50% before cyclin B1. An anti-Emi2 antibody also revealed Emi2 protein in pronucleate embryos, which is in agreement with the observations of Shoji et al. (2006), demonstrating that Emi2 reaccumulates in one-cell embryos and, thus, interestingly, may have a mitotic function. We have previously reported on Ca^{2+} spiking during the first mitotic division of mouse embryos (Kono et al., 1996), suggesting that in this study Emi2 may be degraded by a similar Ca^{2+}-dependent process.

In MetII-arrested mouse oocytes, the APC is already active, but the addition of a Ca^{2+} signal speeds up cyclin B1 degradation sixfold through an increase in APC activity (Nixon et al., 2002). In mouse, the high levels of cyclin B1 required for MetII arrest are therefore achieved through equilibrium between synthesis and degradation (Kubiak et al., 1993). Induction of a spindle-assembly checkpoint by nocodazole prevents cyclin B1 degradation, with or without the presence of a Ca^{2+} signal (Nixon et al., 2002), showing that in mouse oocytes APC activity can be held in check by both CSF and a spindle-assembly checkpoint. In mouse, the spindle-assembly checkpoint is distinct from CSF (Tsurumi et al., 2004). In contrast to cyclin B1, we found little evidence of Emi2 protein turnover in MetII-arrested oocytes, suggesting that Emi2 itself is not a substrate of the APC. Indeed, upon a Ca^{2+} signal, destruction of *X. laevis* Emi2 has been shown to occur via the phosphorylation of a

known SCF$^{\beta\text{-TRCP}}$ (Skp1-Cullin-F-box$^{\beta\text{-TRCP}}$) motif (DSGX$_3$S) and not the APC (Rauh et al., 2005; Tung et al., 2005).

Establishment of MetII arrest

We used a MO antisense oligonucleotide to ablate the Emi2 rise during mouse oocyte maturation and confirmed a knockdown by Western blotting. By blocking the accumulation of Emi2, we have demonstrated that it is essential for stabilizing cyclin B1 after MetI during interkinesis, and therefore essential for the formation of a MetII spindle. Because of the known inhibitory action of Emi2 on APC activity, we interpret this observation to mean that in the absence of Emi2, the APC remains active, and thus cyclin B1 is continuously degraded. In agreement with this is our observation that nondegradable cyclin B1, but not full-length cyclin B1, rescues a MetII arrest after Emi2 knockdown (Fig. 7 vs. Fig. 8), as does the APC^{cdc20} inhibitor Mad2. The current data have not ruled out some effect of Emi2 on cyclin B1 synthesis. However, if so, Emi2 would also be able to negatively regulate expression of the microinjected cyclin B1 cRNA (Fig. 7). This lacks the cyclin B1 gene 3′UTR, which is important for regulating translation through polyadenylation (Tay et al., 2000). Therefore, we would argue that Emi2 is most likely affecting the rate of cyclin B1 degradation, rather than synthesis.

The observed Emi2 MO phenotype, PB1 extrusion and decondensed chromatin within a single pronucleus, was not caused by a nonspecific effect of the MO for two reasons. First, we used two control MOs that were without effect. Second, we rescued the Emi2 knockdown by readdition of Emi2 cRNA, an approach that was made possible by the fact that the rescue cRNA did not contain the 5′UTR recognized by the MO. In some instances, especially where rescue was done with the higher dose of Emi2, oocytes went on to arrest at MetI. This would be consistent with Emi2 inhibiting the APC at this time and the requirement for APC activity in order for mouse oocytes to complete the first meiotic division (Herbert et al., 2003; Terret et al., 2003; Hyslop et al., 2004; Homer et al., 2005). Interestingly, the effect of Emi2 knockdown on oocyte maturation is the same as that obtained when expression of cyclin B1 is prevented by antisense during oocyte maturation (Ledan et al., 2001). In oocytes matured with cyclin B1 antisense, MPF activity is not reestablished after PB1 extrusion, and a single pronucleus forms.

The Emi2 phenotype observed on in vitro–matured oocytes to some extent resembles the siRNA Emi2 knockdown phenotype obtained previously (Shoji et al., 2006), with decondensed chromatin in the parthenote. In that study, however, there was no analysis made of the spindle during the normal time course of maturation; instead, observations were made some 30 h after microinjection. Therefore, in such circumstances it was not possible to judge how the oocyte was progressing through meiosis I, for example if a MetII spindle formed and remained stable for some hours before extruding a PB and exiting meiosis II. Also, the difficulty in interpretation at this single time point was exacerbated in this strain of mouse by the degeneration of the PB1 during the 30-h period.

The present experiments were designed to examine in detail the role of Emi2 during the normal timings of meiosis I.

It was found that Emi2 was essential to restabilize cyclin B1 during interkinesis, and this rise in cyclin B1 was necessary to build a bipolar spindle. This is a previously unreported role for Emi2 in either frog or mouse and may add clarity to the function of CSF in mouse. Given that species-specific differences appear to exist, it is unclear whether this role in establishing MetII arrest would be conserved in frog. In frog, several studies have elegantly identified the c-Mos–MAPK–p90rsk–Bub1 pathway (Sagata et al., 1989; Kosako et al., 1994; Bhatt and Ferrell, 1999; Gross et al., 1999, 2000; Tunquist and Maller, 2003) and the spindle checkpoint proteins Mad1 and Mad2 as essential for the establishment of MetII arrest (Tunquist et al., 2003). Once established, Emi2 contributes to the maintenance of MetII arrest (Liu and Maller, 2005; Rauh et al., 2005; Schmidt et al., 2005; Tung et al., 2005; Hansen et al., 2006), and is perhaps also required for the establishment of MetII arrest; however, this requires further investigation.

When compared with reports in frog, the mechanism of the establishment of MetII arrest in mouse is poorly understood. In contrast to frog, there have been no firm candidates suggested to be involved in establishment. Oocytes from c-Mos −/− mice initially arrest at MetII for 2–4 h, but then fail to maintain this arrest and exhibit spontaneous parthenogenetic activation (Colledge et al., 1994; Hashimoto et al., 1994; Verlhac et al., 1996). Verlhac et al. (1996) demonstrated convincingly that although c-Mos is required for the stabilization of MPF once MetII is achieved, neither c-Mos nor MAPK are involved in MPF reactivation during the MetI–MetII transition. These data suggest that c-Mos is part of the maintenance of MetII arrest, but not its establishment. In agreement with this, the addition of MAPK inhibitors to MetII oocytes induces parthenogenetic activation (Phillips et al., 2002). Therefore, it is clear that the c-Mos–MAPK pathway contributes to MetII arrest once it is established. In any event, MAPK activity declines after cyclin B1 degradation, so MAPK is not targeted immediately by the Ca^{2+} signal at fertilization (Verlhac et al., 1994). Similarly, the main downstream target of MAPK activity in frog appears to have little role in MetII arrest in mouse because oocytes from p90rsk knockout mice (Dumont et al., 2005) still arrest at MetII. Furthermore, oocytes injected with dominant-negative forms of Bub1 and Mad2 still arrest at MetII (Tsurumi et al., 2004), suggesting that spindle checkpoint proteins are not involved in MetII arrest in mouse.

Although not involved in the establishment of MetII arrest, MAPK still appears to have a role in mouse oocytes before the formation of a MetII spindle through a MAPK-interacting and spindle-stabilizing protein (MISS; Lefebvre et al., 2002). MISS is present at meiosis I, but only becomes stable in meiosis II, where it is essential for the maintenance of spindle integrity. Oocytes maturing in the absence of MISS reach MetII arrest, but with severe spindle disorganization, including monopolar spindles, numerous asters in the cytoplasm, or no spindle (Lefebvre et al., 2002). However, because spindle defects in these oocytes are not associated with a drop in cyclin B1 levels or histone H1 activity, it is suggested that MISS does not have a direct role in CSF arrest. Instead, MISS plays a role in microtubule dynamics through an interaction with a microtubule-associated protein.

Previously, all CSF candidates demonstrated in frog appeared to play either no role in CSF activity in mouse or are involved in only the maintenance of arrest once a MetII spindle is established. In this study, we have demonstrated that in the absence of Emi2, mouse oocytes fail to form a bipolar MetII spindle and, thus, fail to establish MetII arrest because of an inability to elevate cyclin B1 levels in interkinesis. Therefore, these data, together with rescue of the Emi2 MO phenotype using exogenous Δ90 cyclin B1 added after PB1 extrusion, imply that the driving force in establishing a bipolar spindle at the end of meiosis is a restabilization of cyclin B1 by Emi2.

Materials and methods

All chemicals were obtained from Sigma-Aldrich, unless otherwise stated, and were of tissue culture or embryo-tested grade where appropriate.

Gamete collection and culture
4–6-wk-old MF1 mice (Harlan) were used. GV oocytes and MetII oocytes were collected from hormonally primed animals, as previously described (Nixon et al., 2002; Hyslop et al., 2004). For bench handling, microinjections, and imaging experiments, GV oocytes and MetII oocytes were cultured in medium M2. When necessary, oocytes were arrested at the GV stage in medium M2 containing 1 μM milrinone. For longer term incubation, GV oocytes and maturing oocytes were held in a 5% CO_2-humidified incubator at 37°C and cultured in MEM (Invitrogen) with 20% fetal calf serum. Parthenogenetic activation of MetII oocytes was achieved by washing oocytes into Ca^{2+}-free M2 media containing 10 mM $SrCl_2$ (Bos-Mikich et al., 1997; Madgwick et al., 2004). Cycloheximide was added to media at a concentration of 10 μg/ml, and nocodazole was added at a concentration of 100 nM. In the case of nocodazole, oocytes were incubated for 15 mins before parthenogenetic activation.

Microinjection and imaging
Microinjection of MOs and cRNA constructs were made as described previously on the heated stage of an inverted microscope (TE300; Nikon) fitted for epifluorescence (Nixon et al., 2002). In brief, fabricated micropipettes were inserted into cells using the negative capacitance overcompensation facility on an electrophysiological amplifier (World Precision Instruments); this procedure ensures a high rate of survival (>90%). Images were recorded using a 20× objective, NA 0.75, and a charge-coupled device camera (Micromax 1300Y; Sony). Filter sets were 430 ±10 nm and 500 ±10 excitation filters for Cerulean and Venus, respectively (Coherent) with a CFP/YFP 51017 BS&M dichroic mirror and emission filter (Chroma Technology Corp.). Hoechst staining was examined using a 360 ±10.9 nm excitation filter (Chroma Technology Corp.). All live cell imaging was performed in medium M2 at 37°C. Confocal sections of Hoechst and Texas red staining were performed on a confocal microscope (SP2; Leica) to capture images of the spindle microtubules and chromatin. MetaMorph and MetaFluor imaging software (Universal Imaging Corp.) were used for image capture and data analysis.

cRNA constructs and MOs
Using primers specifically for the mouse homologue of the Emi2 gene (AK030012; National Center for Biotechnology Information), we amplified full-length mouse Emi2 by PCR from a mouse MetII-arrested oocyte cDNA library. In brief, the cDNA library was prepared by collecting 750 MetII oocytes in sterile PBS. Oocytes were lysed immediately, and mRNA was isolated directly using a commercial kit according to the manufacturers instruction (Dynabeads mRNA Direct kit; Dynal). Double-stranded cDNA was synthesized from RNA and amplified by PCR using a cDNA synthesis kit (SMART PCR cDNA Synthesis kit; CLONTECH Laboratories, Inc.). Mouse Emi2 was then cloned from the cDNA library into a modified pRN3 vector, designed to produce mRNA transcript C-terminally coupled to Venus. Full-length cyclin B1 and Δ90 cyclin B1 were amplified by PCR as previously described (Madgwick et al., 2004). Full-length cyclin B1 was cloned into two modified pRN3 vectors designed to produce mRNA transcripts C-terminally coupled to Venus or Cerulean; Δ90 cyclin B1 was cloned into a nonfluorescent pRN3 vector (Madgwick et al., 2004). Mad2 was manufactured as described in Madgwick et al. (2005). cRNA maximal

stability was conferred in all constructs by the presence of a 5′ globin UTR upstream and both 3′UTR and poly (A)–encoding tracts downstream of the gene. cRNA was synthesized using T3 mMESSAGE mMACHINE (Ambion) and dissolved in nuclease-free water to the required micropipette concentration. An antisense MO (Genetools) was designed to recognize the 5′UTR of Emi2. Two further controls were also designed, the invert of this region and a 5mp (for sequences see Table I). All MOs were used at a micropipette concentration of 2 mM.

Anti-Emi2 antibody purification
An MBP fusion of the human Emi2 N terminus (residues 1–400; hEmi2N) and a GST fusion of the mouse Emi2 N terminus (residues 1–398; mEmi2N) were bacterially expressed and purified using standard protocols, with the exception that all procedures involving GST-mEmi2N were conducted in the presence of 0.01% Triton X-100 to maintain protein solubility. Sera from rabbits immunized against MBP-hEmi2N were screened for immunoblot cross-reactivity toward in vitro-translated mouse Emi2. GST-mEmi2N, immobilized on a column of CNBr-activated Sepharose 4B (17–0430-01; GE Healthcare), was used to affinity purify anti-mEmi2 antibodies from cross-reactive sera. Antibodies were eluted from the column using 100 mM glycine, pH 2.5.

Immunoblotting
For Emi2, lysates from oocytes were incubated overnight with anti-mEmi2 in the range of 2.5 to 10 µg/ml. Nonfat milk (5%) was used as a blocking solution. Anti–rabbit IgG (P0448; DakoCytomation; Figs. 1 and 2; NA934; GE Healthcare; Fig. 4) and ECL Plus (RPN2132; GE Healthcare) were used as secondary detection reagents.

For cyclin B1, lysates from oocytes were incubated overnight with anti-cyclin B1(1:400; Abcam; ab72). Nonfat milk (5%) was used as a blocking solution. Anti–mouse IgG (P0447; DakoCytomation) and ECL Plus were used as secondary detection reagents.

Immunostaining of oocytes
Immunostaining of cyclin B1 was performed as previously described (Reis et al., 2006). In brief, oocytes were fixed and permeabilized by an incubation in 3.7% paraformaldehyde in PBS (30 min), followed by incubation in 3.7% paraformaldehyde, 2% Triton X-100 in PBS (30 min). Fixed oocytes were then washed extensively in 1% PVP and 1% BSA in PBS. For spindle staining, oocytes were incubated with rat anti-tubulin antibody (YL1/2, 1:40, Abcam). 5 µg/ml Texas red conjugated anti–rat goat IgG (Abcam) was used as a secondary antibody. To stain chromatin, oocytes received an additional incubation in 10 µg/ml Hoechst 33258. For cyclin B1 staining, oocytes were incubated with mouse anti-cyclin B1 antibody (1:400; Abcam). TRITC-conjugated anti–mouse rabbit IgG/IgM/IgA was used as a secondary antibody (1:40; DakoCytomation).

References

Abrieu, A., T. Lorca, J.C. Labbe, N. Morin, S. Keyse, and M. Doree. 1996. MAP kinase does not inactivate, but rather prevents the cyclin degradation pathway from being turned on in *Xenopus* egg extracts. *J. Cell Sci.* 109:239–246.

Bhatt, R.R., and J.E. Ferrell Jr. 1999. The protein kinase p90 rsk as an essential mediator of cytostatic factor activity. *Science.* 286:1362–1365.

Blow, J.J., and T.U. Tanaka. 2005. The chromosome cycle: coordinating replication and segregation. Second in the cycles review series. *EMBO Rep.* 6:1028–1034.

Bos-Mikich, A., D.G. Whittingham, and K.T. Jones. 1997. Meiotic and mitotic Ca^{2+} oscillations affect cell composition in resulting blastocysts. *Dev. Biol.* 182:172–179.

Colledge, W.H., M.B.L. Carlton, G.B. Udy, and M.J. Evans. 1994. Disruption of c-mos causes parthenogenetic development of unfertilized mouse eggs. *Nature.* 370:65–68.

Dumont, J., M. Umbhauer, P. Rassinier, A. Hanauer, and M.H. Verlhac. 2005. p90Rsk is not involved in cytostatic factor arrest in mouse oocytes. *J. Cell Biol.* 169:227–231.

Eytan, E., Y. Moshe, I. Braunstein, and A. Hershko. 2006. Roles of the anaphase-promoting complex/cyclosome and of its activator Cdc20 in functional substrate binding. *Proc. Natl. Acad. Sci. USA.* 103:2081–2086.

Fang, G., H. Yu, and M.W. Kirschner. 1998. The checkpoint protein MAD2 and the mitotic regulator CDC20 form a ternary complex with the anaphase-promoting complex to control anaphase initiation. *Genes Dev.* 12:1871–1883.

Glotzer, M., A.W. Murray, and M.W. Kirschner. 1991. Cyclin is degraded by the ubiquitin pathway. *Nature.* 349:132–138.

Gross, S.D., M.S. Schwab, A.L. Lewellyn, and J.L. Maller. 1999. Induction of metaphase arrest in cleaving *Xenopus* embryos by the protein kinase p90Rsk. *Science.* 286:1365–1367.

Gross, S.D., M.S. Schwab, F.E. Taieb, A.L. Lewellyn, Y.-W. Qian, and J.L. Maller. 2000. The critical role of the MAP kinase pathway in meiosis II in *Xenopus* oocytes is mediated by p90Rsk. *Curr. Biol.* 10:430–438.

Hansen, D.V., J.J. Tung, and P.K. Jackson. 2006. CaMKII and Polo-like kinase 1 sequentially phosphorylate the cytostatic factor Emi2/XErp1 to trigger its destruction and meiotic exit. *Proc. Natl. Acad. Sci. USA.* 103:608–613.

Harper, J.W., J.L. Burton, and M.J. Solomon. 2002. The anaphase-promoting complex: it's not just for mitosis any more. *Genes Dev.* 16:2179–2206.

Hashimoto, N., N. Watanabe, Y. Furuta, H. Tamemoto, N. Sagata, M. Yokoyama, K. Okazaki, M. Nagayoshi, N. Takedat, Y. Ikawatll, and S. Aizawai. 1994. Parthenogenetic activation of oocytes in c-mos-deficient mice. *Nature.* 370:68–71.

Herbert, M., M. Levasseur, H. Homer, K. Yallop, A. Murdoch, and A. McDougall. 2003. Homologue disjunction in mouse oocytes requires proteolysis of securin and cyclin B1. *Nat. Cell Biol.* 5:1023–1025.

Homer, H.A., A. McDougall, M. Levasseur, K. Yallop, A.P. Murdoch, and M. Herbert. 2005. Mad2 prevents aneuploidy and premature proteolysis of cyclin B and securin during meiosis I in mouse oocytes. *Genes Dev.* 19:202–207.

Hyslop, L., V. Nixon, M. Levasseur, F. Chapman, K. Chiba, A. McDougall, J. Venables, D. Elliott, and K.T. Jones. 2004. Ca^{2+}-promoted cyclin B1 degradation in mouse oocytes requires the establishment of a metaphase arrest. *Dev. Biol.* 269:206–219.

Jones, K.T. 1998. Ca^{2+} oscillations in the activation of the egg and development of the embryo in mammals. *Int. J. Dev. Biol.* 42:1–10.

Jones, K.T. 2005. Mammalian egg activation: from Ca^{2+} spiking to cell cycle progression. *Reproduction.* 130:813–823.

Knott, J.G., M. Kurokawa, R.A. Fissore, R.M. Schultz, and C.J. Williams. 2005. Transgenic RNA interference reveals role for mouse sperm phospholipase Cζ in triggering Ca^{2+} oscillations during fertilization. *Biol. Reprod.* 72:992–996.

Kono, T., K.T. Jones, A. Bos-Mikich, D.G. Whittingham, and J. Carroll. 1996. A cell cycle-associated change in Ca^{2+} releasing activity leads to the generation of Ca^{2+} transients in mouse embryos during the first mitotic division. *J. Cell Biol.* 132:915–923.

Kosako, H., Y. Gotoh, and E. Nishida. 1994. Mitogen-activated protein kinase kinase is required for the mos-induced metaphase arrest. *J. Biol. Chem.* 269:28354–28358.

Kramer, E.R., C. Gieffers, G. Holzl, M. Hengstschlager, and J.-M. Peters. 1998. Activation of the human anaphase-promoting complex by proteins of the CDC20/Fizzy family. *Curr. Biol.* 8:1207–1210.

Kubiak, J.Z., M. Weber, H. de Pennart, N.J. Winston, and B. Maro. 1993. The metaphase II arrest in mouse oocytes is controlled through microtubule-dependent destruction of cyclin B in the presence of CSF. *EMBO J.* 12:3773–3778.

Ledan, E., Z. Polanski, T.E. Terret, and B. Maro. 2001. Meiotic maturation of the mouse oocyte requires an equilibrium between cyclin B synthesis and degradation. *Dev. Biol.* 232:400–413.

Lefebvre, C., M.E. Terret, A. Djiane, P. Rassinier, B. Maro, and M.-H. Verlhac. 2002. Meiotic spindle stability depends on MAPK-interacting and spindle-stabilizing protein (MISS), a new MAPK substrate. *J. Cell Biol.* 157:603–613.

Liu, J., and J.L. Maller. 2005. Calcium elevation at fertilization coordinates phosphorylation of XErp1/Emi2 by Plx1 and CaMKII to release metaphase arrest by cytostatic factor. *Curr. Biol.* 15:1458–1468.

Lorca, T., F.H. Cruzalegui, D. Fesquet, J.C. Cavadore, J. Mery, A. Means, and M. Doree. 1993. Calmodulin-dependent protein kinase II mediates inactivation of MPF and CSF upon fertilization of *Xenopus* eggs. *Nature.* 366:270–273.

Lorca, T., A. Abrieu, A. Means, and M. Doree. 1994. Ca^{2+} is involved through type II calmodulin-dependent protein kinase in cyclin degradation and exit from metaphase. *Biochim. Biophys. Acta.* 1223:325–332.

Madgwick, S., V.L. Nixon, H.-Y. Chang, M. Herbert, M. Levasseur, and K.T. Jones. 2004. Maintenance of sister chromatid attachment in mouse eggs through maturation-promoting factor activity. *Dev. Biol.* 275:68–81.

Madgwick, S., M. Levasseur, and K.T. Jones. 2005. Calmodulin-dependent protein kinase II, and not protein kinase C, is sufficient for triggering cell-cycle resumption in mammalian eggs. *J. Cell Sci.* 118:3849–3859.

Markoulaki, S., S. Matson, A.L. Abbott, and T. Ducibella. 2003. Oscillatory CaMKII activity in mouse egg activation. *Dev. Biol.* 258:464–474.

Markoulaki, S., S. Matson, and T. Ducibella. 2004. Fertilization stimulates long-lasting oscillations of CaMKII activity in mouse eggs. *Dev. Biol.* 272:15–25.

Masui, Y. 2000. The elusive cytostatic factor in the animal egg. *Nat. Rev. Mol. Cell Biol.* 1:228–232.

Masui, Y., and C.L. Market. 1971. Cytoplasmic control of nuclear behavior during meiotic maturation of frog oocytes. *J. Exp. Zool.* 177:129–145.

Morgan, D.O. 1999. Regulation of the APC and the exit from mitosis. *Nat. Cell Biol.* 1:E47–E53.

Nasmyth, K., and C.H. Haering. 2005. The structure and function of SMC and kleisin complexes. *Annu. Rev. Biochem.* 74:595–648.

Nixon, V.L., M. Levasseur, A. McDougall, and K.T. Jones. 2002. Ca^{2+} oscillations promote APC/C-dependent cyclin B1 degradation during metaphase arrest and completion of meiosis in fertilizing mouse eggs. *Curr. Biol.* 12:746–750.

Peters, J.M. 2002. The anaphase-promoting complex: proteolysis in mitosis and beyond. *Mol. Cell.* 9:931–943.

Phillips, K.P., M.A.F. Petrunewich, J.L. Collins, R.A. Booth, X.J. Liu, and J.M. Baltz. 2002. Inhibition of MEK or cdc2 kinase parthenogenetically activates mouse eggs and yields the same phenotypes as Mos−/− parthenogenotes. *Dev. Biol.* 247:210–223.

Rauh, N.R., A. Schmidt, J. Bormann, E.A. Nigg, and T.U. Mayer. 2005. Calcium triggers exit from meiosis II by targeting the APC/C inhibitor XErp1 for degradation. *Nature.* 437:1048–1052.

Reis, A., H.Y. Chang, M. Levasseur, and K.T. Jones. 2006. APC^cdh1 activity in mouse oocytes prevents entry into the first meiotic division. *Nat. Cell Biol.* 8:539–540.

Runft, L.L., L.A. Jaffe, and L.M. Mehlmann. 2002. Egg activation at fertilization: where it all begins. *Dev. Biol.* 245:237–254.

Sagata, N., N. Watanabe, G.F. Vande Woude, and Y. Ikawa. 1989. The c-*mos* proto-oncogene product is a cytostatic factor responsible for meiotic arrest in vertebrate eggs. *Nature.* 342:512–518.

Saunders, C.M., M.G. Larman, J. Parrington, L.J. Cox, J. Royse, L.M. Blayney, K. Swann, and F.A. Lai. 2002. PLCζ: a sperm-specific trigger of Ca^{2+} oscillations in eggs and embryo development. *Development.* 129:3533–3544.

Schmidt, A., P.I. Duncan, N.R. Rauh, G. Sauer, A.M. Fry, E.A. Nigg, and T.U. Mayer. 2005. *Xenopus* polo-like kinase Plx1 regulates XErp1, a novel inhibitor of APC/C activity. *Genes Dev.* 19:502–513.

Shoji, S., N. Yoshida, M. Amanai, M. Ohgishi, T. Fukui, S. Fujimoto, Y. Nakano, E. Kajikawa, and A. Perry. 2006. Mammalian Emi2 mediates cytostatic arrest and transduces the signal for meiotic exit via Cdc20. *EMBO J.* 25:834–845.

Stricker, S.A. 1999. Comparative biology of calcium signaling during fertilization and egg activation in animals. *Dev. Biol.* 211:157–176.

Tay, J., R. Hodgman, and J.D. Richter. 2000. The control of cyclin B1 mRNA translation during mouse oocyte maturation. *Dev. Biol.* 221:1–9.

Terret, M.E., K. Wassmann, I. Waizenegger, B. Maro, J.M. Peters, and M.H. Verlhac. 2003. The meiosis I-to-meiosis II transition in mouse oocytes requires separase activity. *Curr. Biol.* 13:1797–1802.

Tsurumi, C., S. Hoffmann, S. Geley, R. Graeser, and Z. Polanski. 2004. The spindle assembly checkpoint is not essential for CSF arrest of mouse oocytes. *J. Cell Biol.* 167:1037–1050.

Tung, J.J., D.V. Hansen, K.H. Ban, A.V. Loktev, M.K. Summers, J.R. Adler III, and P.K. Jackson. 2005. A role for the anaphase-promoting complex inhibitor Emi2/XErp1, a homolog of early mitotic inhibitor 1, in cytostatic factor arrest of *Xenopus* eggs. *Proc. Natl. Acad. Sci. USA.* 102:4318–4323.

Tunquist, B.J., and J.L. Maller. 2003. Under arrest: cytostatic factor (CSF)-mediated metaphase arrest in vertebrate eggs. *Genes Dev.* 17:683–710.

Tunquist, B.J., M.S. Schwab, L.G. Chen, and J.L. Maller. 2002. The spindle checkpoint kinase Bub1 and cyclin E/Cdk2 both contribute to the establishment of meiotic metaphase arrest by cytostatic factor. *Curr. Biol.* 12:1027–1033.

Tunquist, B.J., P.A. Eyers, L.G. Chen, A.L. Lewellyn, and J.L. Maller. 2003. Spindle checkpoint proteins Mad1 and Mad2 are required for cytostatic factor–mediated metaphase arrest. *J. Cell Biol.* 163:1231–1242.

Verlhac, M.H., J.Z. Kubiak, H.J. Clarke, and B. Maro. 1994. Microtubule and chromatin behavior follow MAP kinase activity but not MPF activity during meiosis in mouse oocytes. *Development.* 120:1017–1025.

Verlhac, M.H., J.Z. Kubiak, M. Weber, G. Geraud, W.H. Colledge, M.J. Evans, and B. Maro. 1996. Mos is required for MAP kinase activation and is involved in microtubule organization during meiotic maturation in the mouse. *Development.* 122:815–822.

Zachariae, W., and K. Nasmyth. 1999. Whose end is destruction: cell division and the anaphase-promoting complex. *Genes Dev.* 13:2039–2058.